Funnel control for impulsive switched systems

Atiyeh Karimi Pour and Stephan Trenn

***Abstract*— Impulsive switched systems encompass various modes, each exhibiting distinct behaviours. Typically, a switching sequence orchestrates transitions between these modes, where state jumps may occur, potentially undermining output tracking performance or system stability. This work introduces a funnel controller tailored for relative degree one nonlinear impulsive switched systems. Notably, this controller operates solely based on system output without necessitating knowledge of system dynamics. Unlike classical funnel controllers with fixed boundaries, the proposed method dynamically adjusts the funnel boundary for each approaching jump, aiming to preserve adherence to the original boundary. No precise knowledge of jump instances or maps is required; approximate jump intervals and an upper bound for maximum jump height suffice. Theoretical analysis establishes that the error remains within the funnel, facilitating successful reference signal tracking. Performance validation is demonstrated via numerical simulation.**

Table of Notation

Symbol	Description
t_k^-, t_k^+	Time instants immediately before and after k-th jump.
y_k^-, z_k^-, e_k^-	Output, internal states, error values before k-th jump.
y_k^+, z_k^+, e_k^+	Output, internal states, error values after k-th jump.
$Y_k^{\max}, Y_k^{\min}$	Bounds of output in $[\underline{t}_k, \bar{t}_{k+1})$.
$Z_k^{\max}$	Upper bound for internal states norm in $(\underline{t}_k, \bar{t}_{k+1})$.
$\alpha_k^{\max}$	Upper bound for k-th jump height.

I. Introduction

The paper addresses the tracking control of a class of nonlinear impulsive switched systems characterized by a global relative degree of one. Impulsive switched systems are characterized by dynamical equations comprising continuous-time differential equations augmented by discrete jumps at specific impulse instances. Specifically, we consider the following single-input single-output nonlinear impulsive switched system:

$$\begin{aligned} \dot{x}(t) &= F_{\sigma(t)}(t, x(t), u(t)), \quad t \neq t_k, \quad x(t_0^-) = x_0 \in \mathbb{R}^n \\ x(t_k^+) &= E_{\sigma(t_k^+)}(t_k^-, x(t_k^-)), \quad t = t_k, \\ y(t) &= H_{\sigma(t)}(t, x). \end{aligned} \tag{1}$$

Here, the impulse time sequence is defined by the set $\mathcal{T} = \{t_k \mid k \in \mathbb{N}_0, t_k \in \mathbb{R}^+, t_{k+1} > t_k\}$. The switching signal, $\sigma : [t_0, \infty) \to \Sigma := \{1, 2, \ldots, M\}$, indicates the current mode $\sigma(t)$ of the system at time $t \geq t_0$ and the system is assumed to have $M \in \mathbb{N}$ modes. The state, input and output of the system at time $t \geq t_0$ are denoted by $x(t) \in \mathbb{R}^n$, $u(t) \in \mathbb{R}$ and $y(t) \in \mathbb{R}$, respectively. For each mode $m \in \Sigma$, the vector field $F_m : \mathbb{R}^+ \times \mathbb{R}^n \times \mathbb{R} \to \mathbb{R}^n$ defines the flow of the system and $E_m : \mathbb{R}^+ \times \mathbb{R}^n \to \mathbb{R}^n$ represents the jump rule. Furthermore, the output map is denoted by $H_m : \mathbb{R}^n \to \mathbb{R}$. It is noted that even if no impulsive behavior is present in the state, i.e. $E_m(t, x) = x$, then the output may still exhibit jumps due to switching output map.

Hybrid behavior is observed in natural phenomena and engineering systems. Mechanical systems experience sudden velocity changes due to collisions, as in bouncing balls and walking robots [1]. Power electronics, such as buck or boost converters, exhibit switching behavior [2], with abrupt voltage and current transitions during semiconductor switching [3]. In networked control systems, communication delays cause impulsive effects [4].

State jumps degrade performance, causing deviations from equilibrium and increased errors in trajectory tracking. For example, consider system (1) with $F(t, x, 0) = -0.2x$, $H(t, x) = x$, jump map $E(t, x) = 4x$, and jump sequence $\mathcal{T} = \{2.70, 6.30, 8.60\}$. The output in Fig. 1 shows state jumps consistently push states away from equilibrium. Adverse effects include delayed equilibrium, excitation of unwanted modes, movement toward instability, chaotic behavior, and reduced performance in accuracy, efficiency, or desired output.

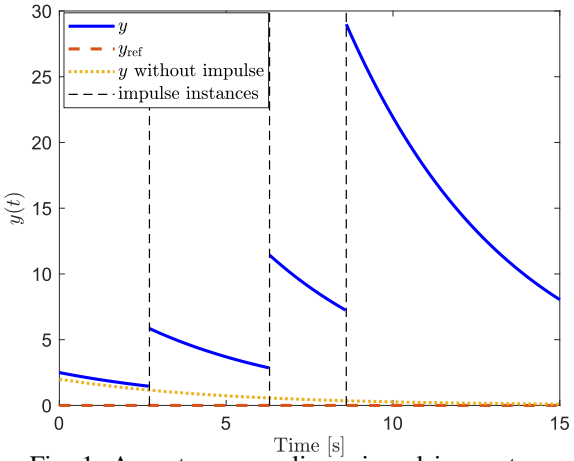

Fig. 1: An autonomous linear impulsive system.

Impulsive switched systems have been extensively studied, for an overview see [5], [6], [7]. Optimal control theory has been applied for disturbance rejection in state-dependent nonlinear impulsive systems, leading to an optimal nonlinear hybrid control law [8], but requiring system model knowledge. Finite-time stability for nonlinear time-dependent im-

A. Karimi Pour is with Bernoulli Institute, University of Groningen, Nijenborgh 9, 9747 AG, Groningen, The Netherlands as a visiting researcher and School of Mechanical Engineering, University of Tehran, 1450 Kargar St. N., Tehran, Iran a.karimi.pour@rug.nl, atiyeh.karimipour@ut.ac.ir

S. Trenn is with Bernoulli Institute, University of Groningen, Nijenborgh 9, 9747 AG, Groningen, The Netherlands s.trenn@rug.nl

pulsive systems was examined in [9], showing stabilizing impulses enhance stability against disturbances, though no specific controller is proposed.

For nonlinear fully-actuated impulsive systems, a high-order fully actuated controller is designed [10], but requires exact system models and full actuation. Sliding mode controllers for stabilizing impulsive systems have been presented in [11], [12], but the focus is on the linear case or restrictive jump sequence assumptions.

In perturbed impulsive systems, LMI-based methods are employed to design a linear state-feedback controller for robust stabilization [13]. A framework for detecting jumps in switched differential-algebraic equations is presented in [14]. An average model for linear impulsive switched systems with pulse width modulation is proposed in [3]. Input-to-State Stability (ISS) conditions for impulsive systems are increasingly studied. ISS of nonlinear impulsive systems under input saturation and disturbance is explored in [15], and event-triggered impulsive control for ISS is investigated under various conditions in [16], [17], [18], [19].

An effective approach to address disturbance impulses within a system is the use of a funnel controller. This controller does not require knowledge of the system model; it only relies on the system's output to track a desired output trajectory. The concept involves defining a performance funnel boundary and designing the control input to ensure that the output tracking error remains within this boundary. This controller enables the characterization of both transient and steady-state behaviour of the output. The only information required about the system is its relative degree. Additional prerequisites include stable internal dynamics and high-gain characteristics. Originally introduced for relative degree one systems in [20], the funnel controller has been extended in numerous directions, see [21] for a recent overview; in particular, this controller has been expanded to systems with higher relative degrees [22], to limit the error derivatives [23], and for achieving synchronization of heterogeneous multi-agent systems using funnel coupling [24], [25].

In this study, we aim to devise a performance funnel to mitigate the adverse effects of impulses and switches. The core idea revolves around adapting the funnel boundary based on estimated jump intervals and the upper bound of jump height, both known a priori, together with decreasing the error as the system approaches the k-th impulse window. Essentially, a narrower local inner funnel with a steeper slope compared to the original funnel is established before each jump interval, to reduce error prior to the jump. Upon the occurrence of a jump, the error either remains within the original funnel (then no further action is necessary) or, if the error jumps outside the funnel, a temporary expansion of the funnel boundary is necessary. However, following a significant jump, the funnel is promptly shrunk back to the desired boundary to restore the desired performance. This approach ensures that the error consistently remains within the (extended) funnel boundary: typically within the desired funnel boundary, and after substantial jumps, within the locally adjusted boundary.

II. Problem formulation

We restrict our attention here to the case of relative degree one and input-affine systems, i.e. we assume that there exists a mode-dependent, nonlinear coordinate change $x \mapsto (y, z)$ such that (1) is equivalent to:

$$\dot{y} = f_{\sigma(t)}(t, y, z) + g_{\sigma(t)}(t, y, z) \cdot u, \qquad t \neq t_k, \quad \text{(2a)}$$

$$y(t_k^+) = J_{\sigma(t_k^+)}(t_k, y(t_k^-), z(t_k^-)), \qquad t = t_k, \quad \text{(2b)}$$

$$\dot{z}(t) = f^z_{\sigma(t)}(t, y, z), \qquad t \neq t_k, \quad \text{(2c)}$$

$$z(t_k^+) = J^z_{\sigma(t_k^+)}(t_k, y(t_k^-), z(t_k^-)), \qquad t = t_k, \quad \text{(2d)}$$

where $z : [t_0, \infty) \to \mathbb{R}^{n-1}$ is the internal state. To ensure existence and uniqueness of local solutions, we assume for each mode $m \in \Sigma$, the functions f_m, J_m, f^z_m, and J^z_m are sufficiently smooth (at least locally Lipschitz continuous).

The proposed controller offers a significant advantage in that it eliminates the requirement for explicit knowledge of the system model, system order, jump map, and the initial value. However, the structure of the system has to have some properties as follows:

(PS1) The system (1) has relative degree one in the sense that it is equivalent to (2).

(PS2) The system has a positive high-frequency gain[1] in the sense that in (2) $g(t, y, z) > 0$ for all t, y, z.

(PS3) The internal dynamics of each mode m of the system is BIBO stable in the sense that there exists a continuous function $\beta_m : \mathbb{R}^+ \times \mathbb{R}^+ \to \mathbb{R}^+$ such that for all continuous y, all solutions of the impulsive switched system (2c) (driven by y as an input) satisfy:

$$\|z(t)\| \leq \beta_{\sigma(t)}(\|y_{[t_k,t)}\|_\infty, \|z(t_k^-)\|), \forall t \in (t_k, t_{k+1}).$$

Furthermore, we assume that there exists a compact set $Z_0 \subseteq \mathbb{R}^{n-1}$, such that $z(t_0^-) = z_0 \in Z_0$.

These features are commonly observed in various real-world systems, including chemical reactors, DC motors, and robotic arms. Additionally, regarding disturbance impulses, the controller doesn't have to have precise information about the exact jump instances and the jump rule; a general understanding of the approximate intervals is sufficient. The assumptions regarding the impulses affecting the system output are outlined below.

(A1) The exact impulse instances are not known, but the controller has access to time intervals within which impulses may occur. In other words, t_k is not known precisely, but it is known that $t_k \in \mathcal{I}_k := [\underline{t}_k, \overline{t}_k]$ for every $k \in \mathbb{N}$. Furthermore, let $\mathcal{I} := \bigcup_{k\in\mathbb{N}} \mathcal{I}_k$. Additionally, the mode sequence of the switching signal is assumed to be known.

(A2) It is supposed that the jump windows do not overlap and have a minimal distance $\Delta t > 0$ from each other, i.e., $\underline{t}_{k+1} - \overline{t}_k \geq \Delta t$.

(A3) Jump rules $J_{\sigma(t)}$ are not explicitly known; however, it is assumed that the jump heights

[1]The term "high-frequency gain" for $g(t, y, z) > 0$ is borrowed from the linear case [21].

are upper-bounded by $|J_m(t_k, y_k^-, z_k^-) - y_k^-| \leq \alpha_{\sigma(t_k^+)}(y_k^-, \|z_k^-\|)\|(y_k^-, z_k^-)\|$, where $\alpha_m : \mathbb{R} \times \mathbb{R}^+ \to \mathbb{R}^+$ is a mode dependent continuous function.

Remark 1: The jump in the output can also occur due to the switching itself, as the output map $H_{\sigma(t)}$ in (1) varies with different modes. It is assumed that the overall jump height, resulting from both the disturbance jump and output map switching, is bounded by the α function in **(A3)**. On the other hand, even if there are no state jumps in the original system (1), the (mode-dependent) coordinate transformation leading to (2) will in general result in jumps in the internal states.

Remark 2: In many real-world systems, jump intervals can often be predicted based on periodic behavior, such as network protocols in control systems or maintenance schedules in mechanical systems. Additionally, designers typically have knowledge of the maximum potential disturbances, which enables the development of control systems capable of managing worst-case scenarios. Consequently, it is not uncommon to establish an upper bound for the jump height.

The desired funnel boundary ψ^{des} and desired output y_{ref} needs to satisfy:

(PB1) $\psi^{\text{des}} : [t_0, \infty) \to (0, \infty)$ is convex, continuously differentiable and has a bounded derivative.

(PB2) The initial error $e(t_0^+) = y(t_0^+) - y_{\text{ref}}(t_0)$ lies within the prescribed funnel, i.e., $|e(t_0^+)| \leq \psi^{\text{des}}(t_0)$.

(PB3) The reference signal $y_{\text{ref}} : [t_0, \infty) \to \mathbb{R}$ is bounded and continuously differentiable, with a bounded derivative.

Convexity of ψ^{des} together with boundedness implies that ψ^{des} is a non-increasing function.

For each jump interval $[\underline{t}_k, \bar{t}_k]$ we specify a "pre-jump" contraction level , $\gamma_k \in (0, \psi^{\text{des}}(\bar{t}_k))$, whose purpose is to reduce the output error in anticipation of an output jump. Employing Assumption **(A3)**, it then becomes feasible to establish an upper bound for the error following each jump. Referring to [23, Lem. 2], it is established that as long as $e(t)$ remains within the funnel, it is possible to determine lower and upper bounds for y. Thus, before the first jump, there exists constants $Y_0^{\max}, Y_0^{\min} \in \mathbb{R}$ such that

$$Y_0^{\max} > \sup_{[t_0, \bar{t}_1)} y_{\text{ref}}(t) + \psi^{\text{des}}(t_0),$$
$$Y_0^{\min} < \inf_{[t_0, \bar{t}_1)} y_{\text{ref}}(t) - \psi^{\text{des}}(t_0).$$

Since the exact value of t_1 is unknown, the supremum and infimum values of y_{ref} within the interval $[t_0, \bar{t}_1)$ is considered. Consequently, before the first jump, the norm of internal dynamic states is also bounded as follows:

$$Z_0^{\max} \geq \max_{y \in [Y_0^{\min}, Y_0^{\max}], z_0 \in Z_0} \beta_{\sigma(t_0^+)}(|y|, \|z_0\|).$$

To determine the maximum possible jump height within this interval, we can choose a constant $\alpha_1^{\max}$ such that:

$$\alpha_1^{\max} \geq \max_{y \in [Y_0^{\min}, Y_0^{\max}], \|z\| \leq Z_0^{\max}} |\alpha_{\sigma(t_1^+)}(y, \|z\|)|.$$

Thus, for the magnitude of the first jump, we have:

$$\begin{aligned} |e_1^+ - e_1^-| &= |y_1^+ - y_1^-| \\ &\leq \alpha_{\sigma(t_1^+)}(y_1^-, \|z_1^-\|)\|(y_1^-, z_1^-)\| \\ &\leq \alpha_1^{\max}(|y_1^-| + \|z_1^-\|) \\ &\leq \alpha_1^{\max}(|e_1^-| + |y_{\text{ref}}(t_1)| + \|z_1^-\|) \\ &\leq \alpha_1^{\max}(|e_1^-| + \sup_{t \in [\underline{t}_1, \bar{t}_1]} |y_{\text{ref}}(t)| + Z_0^{\max}) \\ &\leq C_1(\gamma_1), \end{aligned}$$

where $C_1(\gamma_1) := \alpha_1^{\max}(\gamma_1 + \sup_{t \in [\underline{t}_1, \bar{t}_1]} |y_{\text{ref}}(t)| + Z_0^{\max})$. This bound is valid under the assumption that our controller ensures that the error remains in the desired funnel until the first jump occurs and additionally ensures that $|e_1^-| < \gamma_1$.

The corresponding bounds $C_{k+1}(\gamma_{k+1})$ for all later jump intervals can be determined recursively. Therefore, choose constant $Y_k^{\max}, Y_k^{\min}, Z_k^{\max}, \alpha_{k+1}^{\max}$ such that

$$Y_k^{\max} := \sup_{t \in [\underline{t}_k, \bar{t}_{k+1}]} y_{\text{ref}}(t) + \max(C_k(\gamma_k), \psi^{\text{des}}(\underline{t}_k))$$
$$Y_k^{\min} := \inf_{t \in [\underline{t}_k, \bar{t}_{k+1}]} y_{\text{ref}}(t) - \max(C_k(\gamma_k), \psi^{\text{des}}(\underline{t}_k))$$
$$Z_k^{\max} \geq \max_{y \in [Y_k^{\min}, Y_k^{\max}], \|z\| \leq Z_{k-1}^{\max}} \beta_{\sigma(t_k^+)}(|y|, \|z\|)$$
$$\alpha_{k+1}^{\max} \geq \max_{y \in [Y_k^{\min}, Y_k^{\max}], \|z\| < Z_k^{\max}} |\alpha_{\sigma(t_{k+1}^+)}(y, \|z\|)|$$

and let

$$C_{k+1}(\gamma_{k+1}) := \alpha_{k+1}^{\max}(\gamma_{k+1} + \sup_{t \in [\underline{t}_k, \bar{t}_k]} |y_{\text{ref}}(t)| + Z_k^{\max}) \quad (3)$$

The constant $C_k(\gamma_k)$ represents the maximum jump height at the switching time t_k. It is crucial to note that this value is determined independently of the solution and solely relies on prior available information such as bounds on the reference signal, internal dynamics bounds via β_m, output jump bounds via α_m, jump intervals and mode sequence.

III. Dynamic boundary

Our proposed controller works as follows: As long as there is no upcoming jump, the controller keeps the error inside the desired boundary using a classical funnel controller:

$$k(t) = \frac{1}{\psi(t) - |e(t)|}, \quad (4)$$
$$u(t) = -k(t)e(t), \quad (5)$$

where $\psi(t) = \psi^{\text{des}}(t)$.

However, if a jump is anticipated within the interval $[\underline{t}_k, \bar{t}_k]$, it requires a localized adjustment to the funnel boundary. To achieve this, starting from $\Delta t/2$ seconds before $\underline{t}_k$, the funnel boundary should gradually contract until reaching an appropriate level. The value of Δt is closely tied to the maximum allowable control input that an actuator can deliver. The smaller the permissible control input, the larger the value of Δt needs to be assumed. The extent of height reduction in the funnel boundary during this interval will be discussed later. Consequently, the function describing

this temporary local funnel boundary must possess certain properties outlined in the following definition.

Definition 1: Let $\psi : [t_1, t_2] \to \mathbb{R}$ be a C^1 smooth decreasing function with $\psi(t_1) = a$, $\dot{\psi}(t_1) = b$, $\psi(t_2) = c$, and $\dot{\psi}(t_2) = d$, where $a, b, c, d \in \mathbb{R}$ are given constants with $a > b$ and $c, d \leq 0$. We denote the set of such functions as $\mathcal{F}_{a,b,c,d}^{[t_1,t_2]}$.

Remark 3: An important class of functions belonging to $\mathcal{F}_{a,b,c,d}^{[t_1,t_2]}$ are splines, which can be suitable choices for adjusting funnel boundaries.

The contracting funnel, denoted as ψ_k^{I} and defined in anticipation of the jump at time t_k, is chosen from the set $\mathcal{F}_{a_k^{\mathrm{I}},b_k^{\mathrm{I}},c_k^{\mathrm{I}},d_k^{\mathrm{I}}}^{[\underline{t}_k-\Delta t/2,\underline{t}_k]}$. The parameters within this set are defined as follows. To smoothly guide the error to a lower level, the reduced funnel starts with the same value as the desired funnel at $\underline{t} - \Delta t/2$, then gradually decrease to the specified γ_k over $\Delta t/2$ seconds. Thus:

$$a_k^{\mathrm{I}} = \psi_k^{\mathrm{I}}(\underline{t}_k - \Delta t/2) = \psi^{\mathrm{des}}(\underline{t}_k - \Delta t/2), \tag{6}$$
$$b_k^{\mathrm{I}} = \dot{\psi}_k^{\mathrm{I}}(\underline{t}_k - \Delta t/2) = \dot{\psi}^{\mathrm{des}}(\underline{t}_k - \Delta t/2), \tag{7}$$
$$c_k^{\mathrm{I}} = \psi_k^{\mathrm{I}}(\underline{t}_k) = \gamma_k. \tag{8}$$

During the interval $[\underline{t}_k, t_k)$, the local funnel boundary remains constant at the prescribed level. Therefore, the derivative of ψ_k^{I} at the beginning of the interval is zero.

$$d_k^{\mathrm{I}} = \dot{\psi}_k^{\mathrm{I}}(\underline{t}_k) = 0. \tag{9}$$

Given the upper bound $C_k(\gamma_k)$ of the upcoming jump height, as calculated in (3), the maximum value of the error after the jump is $\gamma_k + C_k(\gamma_k)$. Based on this value, two situations may occur, see also Figure 2.

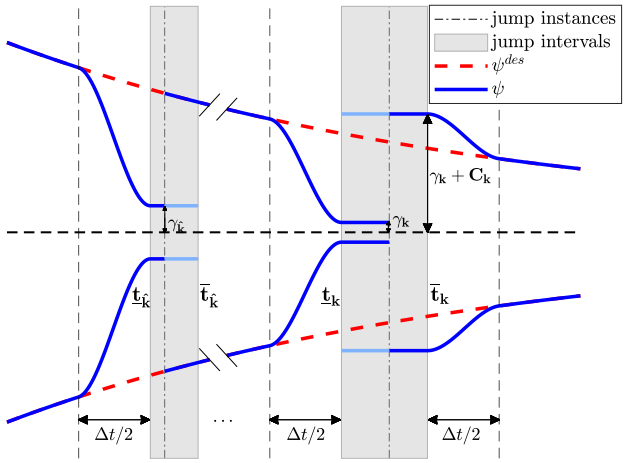

Fig. 2: Adaptive funnel development.

1) $\gamma_k + C_k(\gamma_k)$ is strictly smaller than $\psi^{\mathrm{des}}(\bar{t}_k)$. In that case, the error will remain within the original funnel ψ^{des} after the jump, hence the funnel controller with the original funnel boundary can be used after the jump and no further action is necessary until the next jump. Although the exact time t_k is not known in advance, the jump can be detected simply by observing that the error value suddenly is bigger than γ_k. In case the jump is not detected (because the error after the jumps remains smaller than γ_k), then the funnel switches back to the original funnel at the end of the k-th jump interval.

2) $\gamma_k + C_k(\gamma_k)$ is equal or bigger than $\psi^{\mathrm{des}}(\bar{t}_k)$, we need to expand the boundaries after t_k^+ to the value $\gamma_k + C_k(\gamma_k)$. We keep this value constant until the end of the jump interval and then gradually shrink it back to the original funnel. Although, the exact jump time is not known a-priori, it is trivially detectable by observing that the error left the currently active funnel[2]. Since the boundaries are precomputed, switching to a new boundary incurs no additional computation or delay (as shown by light blue lines in Fig. 2).

To achieve the contraction after the jump interval back to the originally desired funnel, a new function $\psi_k^{\mathrm{II}} \in \mathcal{F}_{a_k^{\mathrm{II}},b_k^{\mathrm{II}},c_k^{\mathrm{II}},d_k^{\mathrm{II}}}^{[\bar{t}_k,\bar{t}_k+\Delta t/2]}$ is defined via:

$$a_k^{\mathrm{II}} = \psi_k^{\mathrm{II}}(\bar{t}_k) = \gamma_k + C_k(\gamma_k), \tag{10}$$
$$b_k^{\mathrm{II}} = \dot{\psi}_k^{\mathrm{II}}(\bar{t}_k) = 0,$$
$$c_k^{\mathrm{II}} = \psi_k^{\mathrm{II}}(\bar{t}_k + \Delta t/2) = \psi^{\mathrm{des}}(\bar{t}_k + \Delta t/2),$$
$$d_k^{\mathrm{II}} = \dot{\psi}_k^{\mathrm{II}}(\bar{t}_k + \Delta t/2) = \dot{\psi}^{\mathrm{des}}(\bar{t}_k + \Delta t/2). \tag{11}$$

By employing an adaptive funnel boundary determined by upcoming jumps, the error consistently remains within the (extended) funnel limits. This result is formalized in the following theorem.

Theorem 1: Consider the nonlinear system described by (2), with an output reference signal $y_{\mathrm{ref}} : \mathbb{R}^+ \to \mathbb{R}$, and a specified desired funnel boundary ψ^{des} satisfying assumptions **(PB1)** to **(PB3)**. Assuming that impulses adhere to the conditions outlined in **(A1)** through **(A3)**, employing the control input defined in (4) and (5), along with the discussed procedure to adjust the funnel boundary, ensures that the error remains within the funnel for all times, i.e., $-\psi(t) < e(t) < \psi(t) \quad \forall t \geq 0$.

Proof: Firstly, it's essential to demonstrate that if the error lies within the funnel before each jump, it will persist within it after the jump by adjusting the funnel boundary using the aforementioned procedure. To illustrate this, in the interval $\mathcal{I}_k$, when $\gamma_k + C_k(\gamma_k) \leq \psi^{\mathrm{des}}(\bar{t}_k)$ (first case), it can be stated:

$$\begin{aligned} |e_k^+| = |e_k^+ + e_k^- - e_k^-| &\leq |e_k^+ - e_k^-| + |e_k^-| \\ &\leq C_k(\gamma_k) + \gamma_k \leq \psi^{\mathrm{des}}(\bar{t}_k). \end{aligned}$$

Note that the maximum value of $|e_k^-|$ before the jump equals to γ_k. Given the monotonicity of $\psi^{\mathrm{des}}(t)$, if $|e_k^+|$ is smaller than $\psi^{\mathrm{des}}(\bar{t}_k)$, it implies that $|e_k^+|$ remains below $\psi^{\mathrm{des}}(t)$ for all $t \in [\underline{t}_k, \bar{t}_k]$.

If $\gamma_k + C_k(\gamma_k) > \psi^{\mathrm{des}}(\bar{t}_k)$ (second case), likewise:

$$|e_k^+| \leq |e_k^+ - e_k^-| + |e_k^-| \leq C_k(\gamma_k) + \gamma_k$$

$C_k(\gamma_k) + \gamma_k$ is equal to the level of adjusted funnel boundary. Now using standard funnel control arguments, we can

[2]In the jump interval, the active funnel is given by the constant γ_k. Note that also in the second case, it can happen that the error after the jump remains in the desired funnel, in that case we can directly use the desired funnel instead of the extended funnel.

conclude that the error stays within the funnel on the interval $[t_k, t_{k+1})$ and the left-limit at t_{k+1} is well defined. ■

Remark 4: It is important to note that with this method, we cannot guarantee that the input will not grow unbounded as $t \to \infty$. This is because the jump maps depend on both the internal dynamics and the output. Specifically, the bound $Z_k^{\max}$ on the internal dynamics depends on the bounds of the outputs $Y_k^{\max/\min}$, which determines the maximal jump height C_{k+1} at the next switching time. This results in larger bounds $Y_{k+1}^{\max/\min}$ and an increased bound $Z_{k+1}^{\max}$ for the internal dynamics, requiring larger inputs to compensate for the internal dynamics and the increasing slope of the adjusted funnel. However, if the upper bound on the jump map is independent of the internal dynamics, such as $\alpha(y)\|y\|$, then the input will not grow unbounded. Finding less conservative conditions which ensure boundedness of the input is a topic of future research.

IV. Simulations

Example 1: This example investigates the system behavior described in Fig. (1) under the implementation of the proposed controller. We analyze the system dynamics defined by $F(t, x, u) = -0.2x + u$. For this example, we set $\gamma_k = \frac{1}{3}\psi^{\text{des}}(\bar{t}_k)$ and $\mathcal{I} = \{[2.00, 3.00], [6.10, 7.00], [8.30, 8.80]\}$. A comparative analysis is performed between the proposed funnel controller and a proportional (P) controller, with the P-controller gain set to $k_p = \{0.4, 1\}$ ($u_p = -k_p e(t)$).

As illustrated in Fig. 3, the funnel controller effectively mitigates the impact of the second and third jumps on the system, with the first jump causing a deviation of 0.14 in y. Additionally, the total control input energy, quantified by $\int_0^t u(t)^2\, dt$, is 101, and the maximum control input is 1.82. Furthermore, for this system and choice of γ_k it can be seen that an extension of the original funnel is not necessary.

For controllers with gains of $k_p = 1$ and $k_p = 0.4$, the total energy consumption and maximum control inputs are 282 and 2.5, and 187 and 1, respectively.

The controller with a gain of $k_p = 0.4$ offers a more comparable energy consumption and maximum control input to the proposed funnel controller. However, as shown in Fig. 3, the output behavior still experiences jumps. Additionally, this controller cannot provide performance guarantees, as the error consistently exceeds the funnel boundaries with each new impulse, and even with closely spaced impulses, the system could become unstable. In contrast, the funnel controller successfully keeps the error within the funnel boundaries.

Example 2. Consider the following nonlinear system with two modes:

Mode 1:

$$\begin{aligned} \dot{y}(t) &= (-z + y + \arctan(y))y + (|y| + 0.25)u, && t \neq t_k \\ y(t_k^+) &= z(t_k^-), && t = t_k \\ \dot{z}(t) &= -z^3 + y \end{aligned}$$

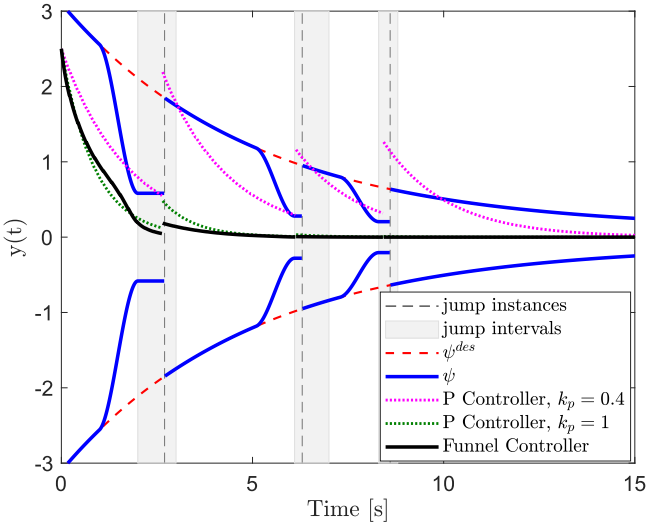

Fig. 3: Comparison of the proposed funnel controller on the system shown in Fig. 1 with proportial controllers with constant gains.

Mode 2:

$$\begin{aligned} \dot{y}(t) &= -2e^y z + 2u && t \neq t_k \\ y(t_k^+) &= y(t_k^-) + z(t_k^-) && t = t_k \\ \dot{z}(t) &= -z - 2z^3 + (1 + z^2)y^2 \end{aligned}$$

The impulse time sequence is given by $\mathcal{T} = \{2.80, 13.37, 23.40\}$ and the jump intervals are $\mathcal{I} = \{[2.48, 3.67], [11.12, 14.58], [21.35, 24.33]\}$. The jump heights in modes one and two are bounded by $|e_k^+ - e_k^-| \leq \sqrt{2}\|(y, z)\|$ and $|e_k^+ - e_k^-| \leq \|(y, z)\|$ respectively. Additionally, the internal state of modes one and two are bounded by $|z(t)| \leq |z_0| + (\|y_{[0,t)}\|_\infty / 0.9)^{1/3}$ and $|z(t)| \leq |z_0| + (\|y_{[0,t)}\|_\infty)^2$ (Cf. [26, p. 177]). Also, $\gamma_k = \frac{10}{18}\psi^{\text{des}}(\bar{t}_k)$ and $\sigma(t) = \{2, 1, 2, 1\}$. Initial conditions are $(y(0), z(0)) = (0.20, 0.05)$ for mode one and $(0.10, 0.10)$ for mode two. Moreover, $y_{\text{ref}} = \sin(t)$, $\psi^{\text{des}} = 2.7e^{-0.15t} + 0.1$ and $\Delta t = 4$s. ψ_k^{I} and ψ_k^{II} are third-order polynomials. The real-time funnel boundary adjustment, the error evolution, and the tracking performance are shown in Fig. 4 and Fig. 5.

As depicted in Figure 4, during the second and third jumps, although the funnel contracts to the level γ_k, the jump height exceeds the desired funnel, leading to an expansion of the funnel boundary after t_k^+. Another noteworthy observation is that the widening of the funnel surpasses the actual jump height. This discrepancy arises due to the unavailability of the actual jump map, necessitating the calculation of the adjusted funnel boundary based on the upper bound of the jump height.

V. Conclusions

A funnel controller for relative degree one nonlinear impulsive switched systems is introduced for tracking reference signals. It does not require knowledge of system model, making it versatile for applications where only output data is available. While exact timing of state jumps during mode

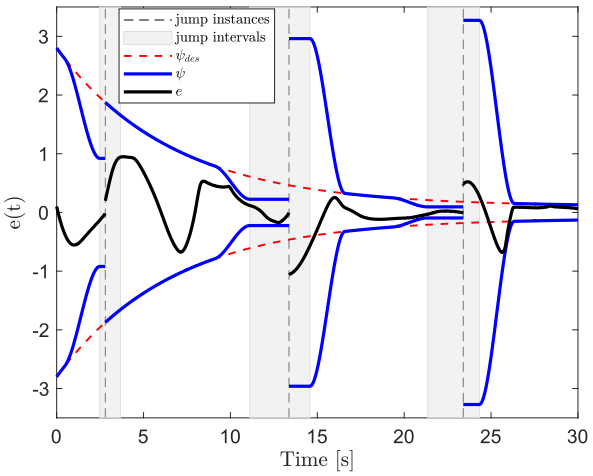

Fig. 4: Evolution of error inside the funnel.

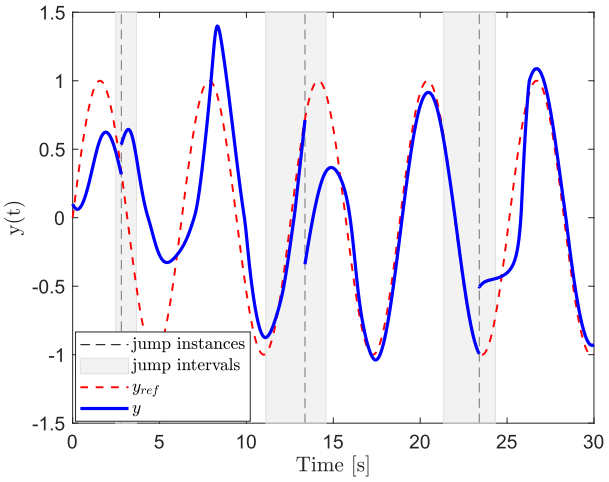

Fig. 5: Output tracking of the controller.

changes isn't needed, knowing the interval for possible switches and the upper bounds of jump heights allows pre-calculation of funnel boundaries. The controller ensures that errors remain within the funnel using classical funnel control inputs. Simulations show effective performance when there is mode switching with disturbance jumps. Future work will explore unbounded input growth, investigate input saturation, and extend the framework to systems with higher relative degrees.

REFERENCES

[1] J. W. Grizzle, G. Abba, and F. Plestan, "Asymptotically stable walking for biped robots: Analysis via systems with impulse effects," *IEEE Transactions on Automatic Control*, vol. 46, no. 1, pp. 51–64, 2001.

[2] C. Albea, G. Garcia, and L. Zaccarian, "Hybrid dynamic modeling and control of switched affine systems: application to dc-dc converters," in *2015 54th IEEE Conference on Decision and Control (CDC)*. IEEE, 2015, pp. 2264–2269.

[3] E. Mostacciuolo, S. Trenn, and F. Vasca, "Averaging for switched impulsive systems with pulse width modulation," *Automatica*, vol. 160, p. 111447, 2024.

[4] M. S. Mahmoud and M. M. Hamdan, "Fundamental issues in networked control systems," *IEEE/CAA Journal of Automatica Sinica*, vol. 5, no. 5, pp. 902–922, 2018.

[5] R. Goebel, R. G. Sanfelice, and A. R. Teel, "Hybrid dynamical systems," *IEEE Control Systems Magazine*, vol. 29, no. 2, pp. 28–93, 2009.

[6] A. Schaft and H. Schumacher, *An introduction to hybrid dynamical systems*. Springer, 2000, vol. 251.

[7] Z. Li, Y. Soh, and C. Wen, *Switched and impulsive systems: Analysis, design and applications*. Springer Science & Business Media, 2005, vol. 313.

[8] W. M. Haddad, N. A. Kablar, V. Chellaboina, and S. G. Nersesov, "Optimal disturbance rejection control for nonlinear impulsive dynamical systems," *Nonlinear Analysis: Theory, Methods & Applications*, vol. 62, no. 8, pp. 1466–1489, 2005.

[9] Y. Xing, X. He, and X. Li, "Lyapunov conditions for finite-time stability of disturbed nonlinear impulsive systems," *Applied Mathematics and Computation*, vol. 440, p. 127668, 2023.

[10] Q. Huang and J. Sun, "Control of impulsive systems via high-order fully actuated system approach," *Nonlinear Dynamics*, vol. 111, no. 19, pp. 17 961–17 971, 2023.

[11] X. Li and Y. Zhao, "Sliding mode control for linear impulsive systems with matched disturbances," *IEEE Transactions on Automatic Control*, vol. 67, no. 11, pp. 6203–6210, 2021.

[12] D. Fan, X. Zhang, and W. Pan, "Sliding mode control for strict-feedback nonlinear impulsive systems with matched disturbances," *IEEE Transactions on Circuits and Systems II: Express Briefs*, 2023.

[13] F. Hao, T. Chu, L. Wang, and L. Huang, "An LMI approach to persistent bounded disturbance rejection for uncertain impulsive systems," in *42nd IEEE International Conference on Decision and Control (IEEE Cat. No.03CH37475)*, vol. 4, 2003, pp. 4068–4073 vol.4.

[14] A. D. Domínguez-García and S. Trenn, "Detection of impulsive effects in switched daes with applications to power electronics reliability analysis," in *49th IEEE Conference on Decision and Control (CDC)*. IEEE, 2010, pp. 5662–5667.

[15] H. Zhu, X. Li, and S. Song, "Input-to-state stability of nonlinear impulsive systems subjects to actuator saturation and external disturbance," *IEEE Transactions on Cybernetics*, 2021.

[16] X. Li, T. Zhang, and J. Wu, "Input-to-state stability of impulsive systems via event-triggered impulsive control," *IEEE Transactions on Cybernetics*, vol. 52, no. 7, pp. 7187–7195, 2021.

[17] M. Cao, Z. Ai, and L. Peng, "Input-to-state stabilization of nonlinear systems via event-triggered impulsive control," *IEEE Access*, vol. 7, pp. 118 581–118 585, 2019.

[18] X. Li, H. Zhu, and S. Song, "Input-to-state stability of nonlinear systems using observer-based event-triggered impulsive control," *IEEE Transactions on Systems, Man, and Cybernetics: Systems*, vol. 51, no. 11, pp. 6892–6900, 2020.

[19] B. Jiang, J. Lu, X. Li, and J. Qiu, "Event-triggered impulsive stabilization of systems with external disturbances," *IEEE Transactions on Automatic Control*, vol. 67, no. 4, pp. 2116–2122, 2021.

[20] A. Ilchmann, E. P. Ryan, and C. J. Sangwin, "Tracking with prescribed transient behaviour," *ESAIM: Control, Optimisation and Calculus of Variations*, vol. 7, pp. 471–493, 2002.

[21] T. Berger, A. Ilchmann, and E. P. Ryan, "Funnel control of nonlinear systems," *Mathematics of Control, Signals, and Systems*, vol. 33, pp. 151–194, 2021.

[22] T. Berger, H. H. Lê, and T. Reis, "Funnel control for nonlinear systems with higher relative degree," *PAMM*, vol. 18, no. 1, p. e201800059, 2018.

[23] J. Hu, S. Trenn, and X. Zhu, "A novel two stages funnel controller limiting the error derivative," *Systems & Control Letters*, vol. 179, p. 105601, 2023.

[24] J. G. Lee, S. Trenn, and H. Shim, "Synchronization with prescribed transient behavior: Heterogeneous multi-agent systems under funnel coupling," *Automatica*, vol. 141, p. 110276, 2022.

[25] J. G. Lee, T. Berger, S. Trenn, and H. Shim, "Edge-wise funnel output synchronization of heterogeneous agents with relative degree one," *Automatica*, vol. 156, no. 111204, pp. 1–10, 2023.

[26] H. Khalil, *Nonlinear Systems*, ser. Pearson Education. Prentice Hall, 2002. [Online]. Available: https://books.google.de/books?id=t_d1QgAACAAJ